

Greedy Part-Wise Learning of Sum-Product Networks

Robert Peharz, Bernhard C. Geiger and Franz Pernkopf

Signal Processing and Speech Communication Laboratory
Graz, University of Technology

Abstract. Sum-product networks allow to model complex variable interactions while still granting efficient inference. However, the learning algorithms proposed so far are explicitly or implicitly restricted to the image domain, either by assuming variable neighborhood or by assuming that dependent variables are related by their values over the training set. In this paper, we introduce a novel algorithm, learning the structure and parameters of sum-product networks in a greedy bottom-up manner. Our algorithm subsequently merges probabilistic models of small variable scope to larger and more complex models. These merges are guided by statistical dependence test, and parameters are learned using a maximum mutual information principle. In experiments we show that our method competes well with the existing learning algorithms for sum-product networks on the task of reconstructing covered image regions, and outperforms these when neither neighborhood nor variable relation by value can be assumed.

1 Introduction

Recently, a new type of probabilistic graphical models called sum-product network (SPN) was proposed [1]. Motivated by arithmetic circuits [2, 3] and aiming at expressive models, still allowing efficient inference, they represent the network polynomial of a Bayesian network [2] with a deep network architecture containing sum and product nodes. In that way, SPNs combine the domains of deep (belief) learning and probabilistic graphical models. On the one hand, SPNs can be interpreted as deep neural networks with sum and product nodes as neurons, where the sum nodes compute a *weighted* sum (with non-negative weights) of its inputs. Besides the network structure, the weights determine the network input-output function, i.e. they represent the parameters of the network. In order to allow efficient inference, the SPN should fulfill certain constraints on the network structure, namely completeness (concerning sum nodes) and consistency or decomposability (concerning product nodes) [1]. On the other hand, SPNs represent Bayesian networks (BNs) with rich latent structure – since sum nodes can be interpreted as hidden variables being summed out – with a high degree of context-specific independence among the hidden variables. The observable variables are placed as leaves of the BN, interacting with each other only via their

latent parents. The BN interpretation opens the door for learning techniques from probabilistic graphical models, such as EM.

In [1], a learning algorithm tailored for image processing was proposed. This algorithm recursively divides an image into pairs of smaller rectangles, and learns the weights of the allotted sum nodes using a kind of hard EM, penalizing the evocation of non-zero weights¹. This algorithm relies on locality of image regions to define the basic SPN structure, and cannot be easily applied to domains without notions of locality. In [5], a hard gradient descent method optimizing the conditional likelihood was proposed, showing convincing results on image classification tasks. The used structure is a 4-layered network on top of a image-feature generation process proposed in [6]. Therefore, also this algorithm is restricted to the image domain. Dennis and Ventura [7] use the same algorithm as in [1] for learning the SPN parameters, but propose an algorithm for finding the basic structure automatically. Their algorithm recursively splits so-called *regions*, i.e. sets of observable random variables, into pairs of smaller regions, using a heuristic application of k -means. This approach clusters variables together which have similar value trends over the dataset. Therefore, also this approach is primarily useful for the image domain, and the prior knowledge about locality is implicitly given by the fact that neighboring pixels typically have similar color values. Furthermore, as the authors note, the application of k -means in this manner is rather unusual and lacks justification.

In this paper, we propose a novel algorithm for learning SPNs, where our structure learning mechanism is well justified and can be applied to discrete random variables, continuous random variables, and mixtures thereof. Our method does *not* rely on explicit or implicit locality assumptions, but learns the SPN structure guided by independence tests and a maximum mutual information principle. It constructs SPNs starting from simple models over small variable scopes, and grows models over larger and larger variable scopes, building successively more expressive models (bottom-up approach). This gives an alternative to the top-down approaches proposed in [1, 7], which determine the SPN structure by recursive splits of variable scopes. Therefore, our method is closer in spirit to traditional training of deep belief networks [8–10], which also aim to extract successively more abstract features in a bottom-up manner.

The paper is organized as follows: In section 2, we introduce our notation and formally review SPNs. In section 3, we introduce our approach for learning SPNs in a bottom-up manner. In section 4, we experimentally show that our method competes well with the existing approaches in the task of image completion, and succeeds them when their assumptions are not met. Section 5 concludes the paper, and gives possible directions for future work.

¹ The claimed ℓ^0 -norm penalization in [1] is not truly implemented in the provided software [4], since already evoked non-zero weights are *not* penalized any more.

2 Background and Notation

Assume a set of random variables (RVs) $\mathbf{X} = \{X_1, \dots, X_D\}$, where each X_d can take values out of the set $\mathbf{val}(X_d) \subseteq \mathbb{R}$. When $\mathbf{val}(X_d)$ is finite, we say that X_d is *discrete*. In this case, inputs concerning X_d are represented using $|\mathbf{val}(X_d)|$ binary *indicator* nodes. When $\mathbf{val}(X_d)$ is infinite, inputs can be represented by *distribution* nodes (e.g. Gaussian). For now, let us assume that all RVs are discrete. Let $x_d^j \in \mathbf{val}(X_d)$ be the j^{th} state of X_d , and I_d^j be the corresponding indicator node, which can assume values out of $\{0, 1\}$.

An SPN structure [1] is defined as a connected acyclic directed graph, whose leaves are the indicator nodes for RVs \mathbf{X} , and all non-leaves are either *sum* or *product* nodes. The value of a product node is the product of values of its child nodes. The values of a sum node is the *weighted* sum of the values of its child nodes, where the weights are non-negative parameters. We assume SPNs which are organized layer-wise, i.e. sum and product layers alternate when proceeding to higher layers. Furthermore, the first layer is an input layer, the second is a product layer and the last (output) layer is a sum layer. The alternation of sum and product layers does not restrict generality, since both a sum node and a product node can be used to reproduce the value of a child node of a preceding layer. We assume that nodes are allowed to receive input only from a strictly lower layer. This assumption does not restrict generality either, since the SPN structure is per definition acyclic, and can always be organized in a feed-forward structure. We call these SPNs (organized in layers and feed-forward) *layered* SPNs.

We have L sum and L product layers, such that in total the SPN contains $2L + 1$ layers, where the first layer is the input layer, containing the indicator (or distribution) nodes. Let P^l be the l^{th} product layer (the $(2l)^{\text{th}}$ layer in the SPN), and S^l the l^{th} sum layer (the $(2l + 1)^{\text{th}}$ layer in the SPN). Let S_k^l be the k^{th} sum node in the l^{th} sum layer, and like-wise P_k^l for product layers. In graphical representations of the SPN structure, we assume that nodes within one layer are numerated from left to right. The *parents* of a generic node N are denoted as $\text{pa}(N)$, and the children are denoted as $\text{ch}(N)$. Let the *scope* $\text{sc}(N)$ of a node be a sub-set of the index set $\{1, \dots, D\}$ for RVs \mathbf{X} . For an indicator node I_d^j , the scope is defined as $\text{sc}(I_d^j) = \{d\}$. For sum and product nodes, the scope is recursively defined as $\text{sc}(N) = \bigcup_{C \in \text{ch}(N)} \text{sc}(C)$. Let $\mathbf{X}_{\text{sc}(N)}$ be the sub-set of \mathbf{X} which is indexed by $\text{sc}(N)$. A *root* is a node R with $\text{pa}(R) = \emptyset$. In [1, 7], only SPNs with a single root R were considered, and where $\text{sc}(R) = \{1, \dots, D\}$. In this paper, we also strive for SPNs with a single root, representing the full variable scope; however, as intermediate step, we will consider also SPNs with multiple roots, and also roots whose scope is a strict sub-set of $\{1, \dots, D\}$ (see section 3). For now, we assume SPNs with a single root R . A *sub-SPN* induced by some node N is the SPN defined by the sub-graph induced by N and all its descendants, including the corresponding parameters. N is the (single) root of its induced sub-SPN.

Let $\mathbf{e} = (e_1^1, \dots, e_1^{|\text{val}(X_1)|}, \dots, e_D^1, \dots, e_D^{|\text{val}(X_D)|})$ denote some input to the SPN, i.e. a binary pattern for the indicator nodes. Let $N(\mathbf{e})$ denote the *value* of node N for input \mathbf{e} . For indicator nodes, $I_d^j(\mathbf{e}) = e_d^j$. To input *complete* evidence, i.e. a variable assignment $\mathbf{x} = (x_1, \dots, x_D)$ to the SPN, the value indicator node are set $e_d^j = 1$ if $x_d = x_d^j$, and $e_d^j = 0$ otherwise. When \mathbf{e} encodes some complete evidence \mathbf{x} , we write $\mathbf{e} \sim \mathbf{x}$, and also use $N(\mathbf{x})$ for $N(\mathbf{e})$. The values for sum and product nodes are determined by an upward pass in the network.

The root-value $R(\mathbf{x})$ is the *output* of an SPN for assignment \mathbf{x} . An SPN defines the probability distribution

$$P(\mathbf{x}) := \frac{R(\mathbf{x})}{\sum_{\mathbf{x}' \in \text{val}(\mathbf{X})} R(\mathbf{x}')}. \quad (1)$$

While (1) can also be defined for standard neural networks, SPNs become truly powerful when they are *valid* [1], which means that for all state collections $\xi_d \subseteq \text{val}(X_d)$, $d \in \{1, \dots, D\}$, it holds that

$$\sum_{x_1 \in \xi_1} \cdots \sum_{x_D \in \xi_D} P(x_1, \dots, x_D) = \frac{R(\mathbf{e})}{\sum_{\mathbf{x}' \in \text{val}(\mathbf{X})} R(\mathbf{x}')}, \quad (2)$$

where now $e_d^j = 1$ if $x_d^j \in \xi_d$, and otherwise $e_d^j = 0$. In words, a valid SPN allows to efficiently marginalize over *partial* evidence by a single upward pass. The efficient marginalization in SPNs stems from a compact representation of the network polynomial of an underlying Bayesian network [1, 2]. Poon and Domingos [1] give sufficient conditions for the validity of an SPN, namely *completeness* and *consistency*:

Definition 1. *An SPN is complete, if for each sum node S all children of S have the same scope.*

Definition 2. *An SPN is consistent, if for each product node P and each two of its children $C, C' \in \text{ch}(P)$, $C \neq C'$, it holds that when an indicator I_d^j is a descendant of C , no indicator $I_d^{j'}$, $j \neq j'$, is a descendant of C' .*

Completeness and consistency are sufficient, but not necessary for validity; however, these conditions are necessary when also every sub-SPN rooted at some node N should be valid [1]. Definition 2 is somewhat cumbersome, and it is also questionable how consistency should be interpreted in the case of continuous RVs. Therefore, Poon and Domingos provide a simpler and more restrictive condition, which implies consistency, namely decomposability:

Definition 3. *An SPN is decomposable, if for each product node P and each two of its children $C, C' \in \text{ch}(P)$, $C \neq C'$, it holds that $\text{sc}(C) \cap \text{sc}(C') = \emptyset$.*

Finally, we illustrate how continuous data can be modeled using SPNs. Following [1], one can simply use *distribution nodes* (instead of indicator nodes) for continuous RVs, e.g. with nodes returning the value of a Gaussian PDF (Gaussian nodes) as output. A simple example, showing a 4-component GMM with

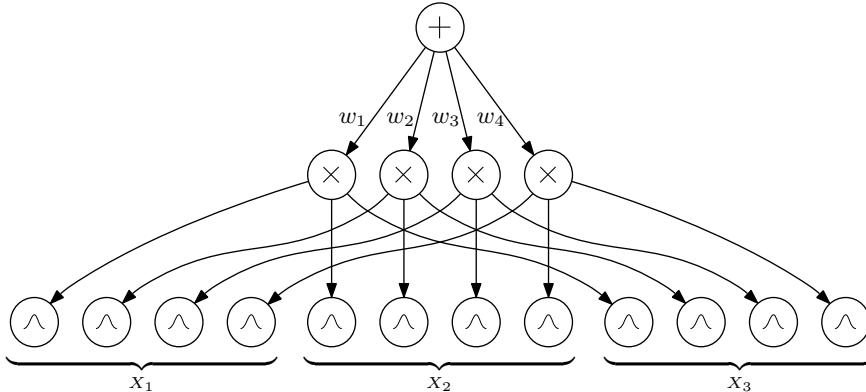


Fig. 1. SPN representing a Gaussian mixture model over three variables X_1, X_2, X_3 with 4 components and diagonal covariance matrix. The component priors (sum weights) are w_1, w_2, w_3, w_4 , satisfying $w_1 + w_2 + w_3 + w_4 = 1$, $w_1, w_2, w_3, w_4 \geq 0$.

diagonal covariance matrix, is shown in Fig. 1. The parameters of the Gaussians, mean and variance, are considered as parameters of the Gaussian nodes in the input layer and are not shown in the figure.

3 Greedy Part-Wise Learning of SPNs

In this section, we present our approach for part-wise learning of SPNs, where as in [1, 7], we restrict ourselves to complete and decomposable SPNs. We start with some observations serving as guidelines for our approach. First of all, an SPN with a single root R defines a probability distribution over $\mathbf{X}_{\text{sc}(R)}$ according to (1). Consequently, an SPN with multiple roots R_1, \dots, R_r defines *multiple* probability distributions over $\mathbf{X}_{\text{sc}(R_1)}, \dots, \mathbf{X}_{\text{sc}(R_r)}$, respectively, where in general scopes $\text{sc}(R_i)$ and $\text{sc}(R_j)$, $i \neq j$, can differ from each other. The representations of these distributions potentially share computational resources (i.e. intermediate calculations) and parameters. For example, the (complete and decomposable) SPN in Fig. 2 has 4 roots, where the roots S_1^2 and S_2^2 represent two (in general distinct) distributions over the whole scope $\{X_1, X_2, X_3\}$, and roots S_3^1 and S_4^1 represent distributions over scope $\{X_2, X_3\}$. Furthermore, we see that each sub-SPN is again an SPN over the scope $\text{sc}(N)$, where in the simplest case an SPN consists of a single node in the input layer. We call these single-node SPNs *atomic* SPNs. In Fig. 2, all atomic SPNs are indicator nodes². However, as already shown in section 2, atomic SPNs are not restricted to be indicator nodes, but can also be distribution nodes. Even further, atomic SPNs can be probability models with arbitrarily large scopes, not only modeling single variables – they are merely not represented as SPNs in this framework, but represent some external

² An indicator node I_d^j is an SPN, which represents the distribution assigning all probability mass to the event $X_d = x_d^j$.

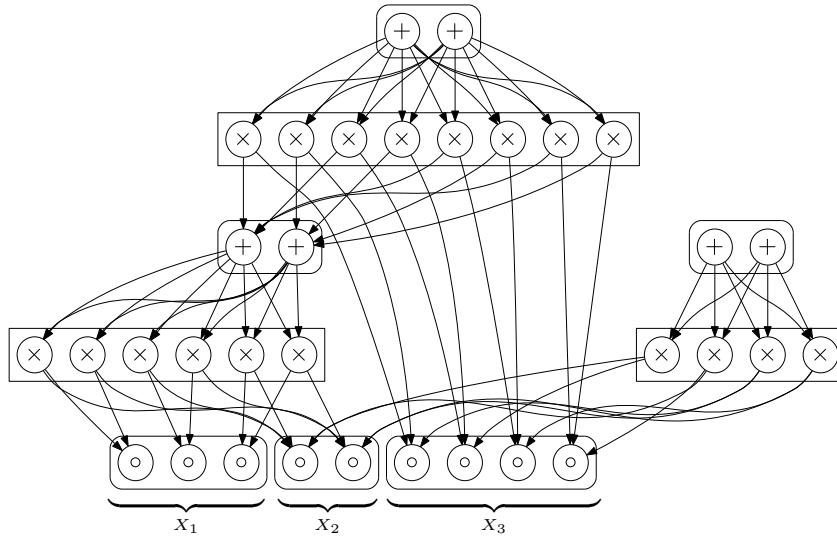


Fig. 2. Example of a multi-root SPN over variables X_1 , X_2 , X_3 with 3, 2 and 4 states, respectively. Nodes with \circ denote indicator nodes. For simplicity, weights of sum nodes are omitted.

“input”-probabilistic models. Product nodes represent distributions which assume *independence* between the variable sets indexed by their child nodes. Sum nodes represent *mixtures of distributions* represented by product nodes. We recognize that larger SPNs are simply *composite smaller* SPNs, where the basis of this inductive principle are atomic SPNs.

Using this interpretation of multi-root SPNs, we can define the *trivial* multi-root SPN which merely contains atomic nodes. Fig. 3 shows the trivial SPN for the same RVs as in Fig. 2. This SPN consists merely of the indicator nodes of

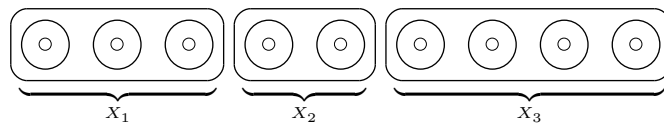


Fig. 3. Most simple multi-root SPN over variables X_1 , X_2 , X_3 with 3, 2 and 4 states, respectively.

X_1 , X_2 , X_3 , which are at the same time roots *and* atomic distributions. The key idea of our approach is to start from the trivial SPN containing only atomic distributions, and generate larger and larger SPNs with successively increasing scope, until we eventually obtain an SPN whose root has a scope over all RVs

\mathbf{X} we aim to model. In this paper, the final model will have a single root, where as intermediate step a series of multi-root SPNs is generated.

To make our approach precise, we adopt the notion of *regions*, *partitions*, and *region graphs* [7], which represents SPNs on a larger scale. The notion of a region is inspired by image modeling, i.e. when RVs \mathbf{X} are the pixel values of an image. However, while adopting terminology, the approach developed here is not necessarily restricted to the image domain.

Definition 4. *Given a layered, complete and decomposable SPN, the region \mathcal{R} with scope $\text{sc}(\mathcal{R}) \subseteq \{1, \dots, D\}$ is the set of atomic or sum nodes, which have all the same scope $\text{sc}(\mathcal{R})$. Regions containing only atomic nodes (e.g. indicator or distribution nodes) are called atomic regions. Regions containing only sum nodes are called composite regions.*

In this paper, we assume for simplicity that regions are either atomic or composite, i.e. they do not contain atomic nodes and sum nodes simultaneously. This restriction, however, is not essential, since we could model a region both with “external” atomic models and with composite smaller models, i.e. with SPNs. For some scope s , we define $\mathcal{R}(s)$ as the region \mathcal{R} with scope s , i.e. $\text{sc}(\mathcal{R}(s)) = s$. While two SPN nodes can have the same scope, regions per definition have a *unique* scope. Regions can be interpreted as *dictionaries* of distributions over the same scope $\text{sc}(\mathcal{R})$. In Fig. 2 and Fig. 3, regions are depicted as boxes with rounded corners. We now define partitions [7], which describe the decomposition of (parent) regions into smaller disjoint (child) regions.

Definition 5. *Given a layered, complete and decomposable SPN, let \mathcal{R}_p be a region and \mathcal{R}_c be a set of disjoint regions, i.e. $\text{sc}(\mathcal{R}) \cap \text{sc}(\mathcal{R}') = \emptyset, \forall \mathcal{R}, \mathcal{R}' \in \mathcal{R}_c, \mathcal{R} \neq \mathcal{R}'$, and where $\text{sc}(\mathcal{R}_p) = \bigcup_{\mathcal{R} \in \mathcal{R}_c} \text{sc}(\mathcal{R})$. The partition $\mathcal{P}(\mathcal{R}_p, \mathcal{R}_c)$ is the set of product nodes whose parent nodes are all contained in \mathcal{R}_p , and which have exactly one child in each $\mathcal{R} \in \mathcal{R}_c$. The scope of a partition $\text{sc}(\mathcal{P}(\mathcal{R}_p, \mathcal{R}_c))$ is defined as $\text{sc}(\mathcal{R}_p)$.*

Note that since we only consider layered, complete and decomposable SPNs, each product node has to be contained in *exactly one partition*. Partitions do *not* have a unique scope, since each parent region \mathcal{R}_p can be composed by several *different* partitions. We define the set of product nodes $\mathcal{P}(\mathcal{R}_p) := \bigcup \mathcal{P}(\mathcal{R}_p, \cdot)$, which contains all product nodes with same scope. In Fig. 2 and partitions are depicted as boxes with edged corners. A *region graph* is defined as follows.

Definition 6. *Given a layered, complete and decomposable SPN; the region graph \mathcal{G} of this SPN is a bipartite directed acyclic graph, with two distinct set of nodes \mathcal{R} and \mathcal{P} , where \mathcal{R} are all non-empty regions and \mathcal{P} are all non-empty partitions of the SPN. Region nodes are connected only with partition nodes, and vice versa. $\mathcal{R} \in \mathcal{R}$ is a parent region of $\mathcal{P}(\mathcal{R}_p, \mathcal{R}_c)$ if and only if $\mathcal{R} = \mathcal{R}_p$. $\mathcal{R} \in \mathcal{R}$ is a child region of $\mathcal{P}(\mathcal{R}_p, \mathcal{R}_c)$ if and only if $\mathcal{R} \in \mathcal{R}_c$.*

Using the notion of a region graph, we can define the *parts* of a region.

Definition 7. Let \mathcal{G} be the region graph of a layered, complete and decomposable SPN. The parts of a region $\mathcal{R} \in \mathcal{G}$ is the set of regions

$$\text{parts}(\mathcal{R}) := \{\mathcal{R}' | \exists \mathcal{P}(\mathcal{R}, \mathcal{R}_c) \in \mathcal{G} : \mathcal{R}' \in \mathcal{R}_c\}. \quad (3)$$

We are now ready to sketch our general approach, which is shown in Algorithm 1. Algorithm 1 starts with the trivial multi-root SPN containing only

Algorithm 1 General Merge Learning

- 1: **Initialization:** Make trivial SPN and corresponding region graph \mathcal{G} .
 - 2: **while** stopping criterion not met **do**
 - 3: **Select Merge Candidates:** Select set of $A \geq 2$ disjoint regions $\mathcal{R}_c = \{\mathcal{R}_{c,1}, \dots, \mathcal{R}_{c,A}\}$, with $\forall a \mathcal{R}_{c,a} \in \mathcal{G}$ and $\mathcal{P}(\mathcal{R}_p, \mathcal{R}_c) \notin \mathcal{G}$, where $\mathcal{R}_p := \mathcal{R}(\bigcup_{a=1}^A \text{sc}(\mathcal{R}_{c,a}))$.
 - 4: **Select Set of Features** $\mathcal{F} \subseteq \mathcal{R}_{c,1} \times \dots \times \mathcal{R}_{c,A}$.
 - 5: $\mathcal{P}_{\text{tmp}} \leftarrow \emptyset$.
 - 6: **if** \mathcal{R}_p already contains sum nodes **then**
 - 7: $\mathcal{P}_{\text{tmp}} \leftarrow \bigcup_{S \in \mathcal{R}_p} \text{ch}(S)$.
 - 8: **end if**
 - 9: Delete all nodes in \mathcal{R}_p .
 - 10: Generate K sum nodes S_k , $k = 1, \dots, K$.
 - 11: **for** $f =: (N_1, \dots, N_A) \in \mathcal{F}$ **do**
 - 12: Generate product node P_f .
 - 13: Connect P_f as parent of N_a , $a = 1, \dots, A$.
 - 14: Connect P_f as child of S_k , $k = 1, \dots, K$.
 - 15: **end for**
 - 16: Connect each product node in \mathcal{P}_{tmp} as child of S_k , $k = 1, \dots, K$.
 - 17: Update region graph \mathcal{G} .
 - 18: **Recursively learn parameters of \mathcal{R}_p and of its ancestor regions.**
 - 19: **end while**
-

atomic regions. In each iteration, some disjoint regions \mathcal{R}_c are selected and merged into a parent region \mathcal{R}_p , generating a new partition $\mathcal{P}(\mathcal{R}_p, \mathcal{R}_c)$. Note that while in each iteration a partition $\mathcal{P}(\mathcal{R}_p, \mathcal{R}_c)$ is newly generated, i.e. it was not in the region graph beforehand, the region \mathcal{R}_p might already have been generated by an earlier merge. As in [1, 7], a collection of sum nodes, one from each child region, is combined by product nodes. Here, a particular selection of child region nodes is called a *feature* (cf. step 4), where each feature corresponds to a product node (cf. steps 11–14). The number of generated sum nodes K will be typically $K \ll |\mathcal{F}|$, i.e. the sum nodes *represent a compression* of the generated features. The quality of this compression depends on the parameter learning in step 18. Since \mathcal{R}_p might have been already existing in the region graph, also its ancestor regions need to be retrained in a recursive upwards pass.

Algorithm 1 describes a general scheme for greedy part-wise learning of SPNs. Depending on the strategy of selecting the merge candidates in step 3, of selecting appropriate features in step 4, and of learning parameters in step 18, we

obtain different learning algorithms. Further questions are to select K and the stopping criterion. We treat these questions in the following sub-sections, where our approach is guided by the concept of *winner* variables. Consider an intermediate multi-root SPN. For each region \mathcal{R} in the corresponding region graph we define a winner variable

$$W_{\mathcal{R}} := W_{\mathcal{R}}(\mathbf{X}) = \arg \max_{i: N_i \in \mathcal{R}} N_i(\mathbf{X}), \quad (4)$$

where we assume some arbitrary ordering of the nodes in \mathcal{R} . As already noted, a region can be interpreted as dictionary of distributions over the same scope. The variable $W_{\mathcal{R}}(\mathbf{x})$ is the indicator of the distribution in \mathcal{R} which describes $\mathbf{X}_{\text{sc}(\mathcal{R})}$ best for sample \mathbf{x} , since the corresponding node represents the model with *highest-likelihood*. With respect to some multi-root SPN, each variable $W_{\mathcal{R}}$ represents some *abstract* information of variables $\mathbf{X}_{\text{sc}(\mathcal{R})}$. The goal in our approach is to preserve and to abstract this information, when proceeding to higher SPN levels.

3.1 Selecting Merge Candidates

We now discuss how to select merge candidates in step 3 of Algorithm 1. Similar as in [1, 7] we set $A = 2$, i.e. we consider decompositions of a parent-region into two sub-regions. The focus for selecting merge candidates is twofold: (i) we aim to find merge candidates which are “advantageous”, and (ii) we want to pursue a merging strategy which yields quickly an SPN with complete scope $\{1, \dots, D\}$, i.e. which models all variables in \mathbf{X} . When we neglect the latter point, our algorithm will typically exhaust memory and overfit the SPN, since there are $2^D - 1$ regions, and the number of partitions for a specific parent region grows exponentially in its size. About the first point, to decide when a merge is advantageous, we use independence tests, which are also used for learning BN structures [11]. In BNs, an edge between two variables should be present when they are statistically dependent. The major criticism about this method is the unreliability of statistical (in)dependence tests, which either causes unreliable models, or models with high inference cost. In SPNs, the variables to be modeled are not directly connected by edges, but their interaction happens over latent parents. Here the unreliability of statistical dependence tests do not harm as much as in BNs, since introducing a new, possibly spurious partition, does increase the inference cost only marginally.

Specifically, we use the Bayesian-Dirichlet independence test proposed in [12], for two winner variables $W_{\mathcal{R}'}$ and $W_{\mathcal{R}''}$:

$$\text{BD}(W_{\mathcal{R}'}, W_{\mathcal{R}''}) = \frac{\frac{\Gamma(\gamma)}{\Gamma(\gamma+M)} \prod_{k=1}^{|\mathcal{R}'|} \prod_{l=1}^{|\mathcal{R}''|} \frac{\Gamma(\gamma_{k,l} + c_{k,l})}{\Gamma(\gamma_{k,l})}}{\left(\frac{\Gamma(\alpha)}{\Gamma(\alpha+M)} \prod_{k=1}^{|\mathcal{R}'|} \frac{\Gamma(\alpha_k + a_k)}{\Gamma(\alpha_k)} \right) \left(\frac{\Gamma(\beta)}{\Gamma(\beta+M)} \prod_{l=1}^{|\mathcal{R}''|} \frac{\Gamma(\beta_l + b_l)}{\Gamma(\beta_l)} \right)}. \quad (5)$$

Here a_k , b_l are the number of times, counted over all training samples, where $W_{\mathcal{R}'}$ and $W_{\mathcal{R}''}$ are in their k^{th} and l^{th} states, respectively, and $c_{k,l}$ is the number

of times where $W_{\mathcal{R}'}$ and $W_{\mathcal{R}''}$ are jointly in their k^{th} and l^{th} states. α_k , β_l , and $\gamma_{k,l}$ are Dirichlet priors, here uniformly set to 1, and $\alpha = \sum_k \alpha_k$, $\beta = \sum_l \beta_l$ and $\gamma = \sum_{k,l} \gamma_{k,l}$. M is the number of samples in the data set. The lower $\text{BD}(W_{\mathcal{R}'}, W_{\mathcal{R}''})$, the more the winner variables $W_{\mathcal{R}'}$, $W_{\mathcal{R}''}$ are dependent, and the more \mathcal{R}' and \mathcal{R}'' “prefer” to merge. To encourage a quick growing of the SPN regions, we use the scheme shown in Algorithm 2. This selection scheme

Algorithm 2 Select Regions

- 1: **if** Select Regions is called the first time or $|\mathcal{M}| = 1$ **then**
 - 2: $\mathcal{M} \leftarrow$ set of all atomic regions.
 - 3: **end if**
 - 4: Select $\mathcal{R}_c = \{\mathcal{R}', \mathcal{R}''\} \in \mathcal{M}$ which minimize $\text{BD}(W_{\mathcal{R}'}, W_{\mathcal{R}''})$, s.t. $\mathcal{P}(\mathcal{R}_p, \mathcal{R}_c) \notin \mathcal{G}$.
 - 5: $\mathcal{M} \leftarrow \mathcal{M} \setminus \mathcal{R}_c$
 - 6: $\mathcal{M} \leftarrow \mathcal{M} \cup \mathcal{R}(\text{sc}(\mathcal{R}') \cup \text{sc}(\mathcal{R}''))$
 - 7: Return $\mathcal{R}_c = \{\mathcal{R}', \mathcal{R}''\}$.
-

maintains a set of merging candidates \mathcal{M} , which is initialized with the disjoint atomic regions. In each iteration of Algorithm 1, the two most dependent regions (by means of (5)) are selected from \mathcal{M} and merged to a parent region. The two selected regions are excluded from the merging candidates \mathcal{M} and the parent region is inserted. In this way, the generated region graph is guaranteed to be a binary tree. When $\mathcal{M} = 1$, i.e. when the root region has been reached, we start the process again, i.e. \mathcal{M} is reset to the set of all atomic regions. Then a parallel, interleaved binary tree is grown, where the constraint $\mathcal{P}(\mathcal{R}_p, \mathcal{R}_c) \notin \mathcal{G}$ guarantees that this tree is different from the first tree. This process, growing interleaved binary trees, is repeated for several iterations (*tree-growing* iterations), where the maximal number of iterations specifies a stopping criterion for Algorithm 1 (step 2). Note that due to the constraint $\mathcal{P}(\mathcal{R}_p, \mathcal{R}_c) \notin \mathcal{G}$ it can happen that in later iterations no more merging candidates can be found in step 4 of Algorithm 2. In this case, we also stop Algorithm 1.

3.2 Selecting Features and Learning Parameters

We now turn to the problem of selecting features and learning parameters in Algorithm 1. The most general approach for selecting features \mathcal{F} would be to take the Cartesian product of the node sets $\{\mathcal{R}_{c,a}\}_{a=1,\dots,A}$, which for $A = 2$ grows quadratically in the number of nodes in the child regions. We reduce this number and use $\mathcal{F} = \{f = (N_k, N_l) | c_{k,l} > 0\}$, where $c_{k,l}$ is defined in (5). In words, we select those features, whose corresponding product node *wins* at least once against all other potential product nodes. As already noted, $K = |\mathcal{R}_p| \ll |\mathcal{F}| = |\mathcal{P}(\mathcal{R}_p)|$ in Algorithm 1, so the sum nodes in \mathcal{R}_p represent a compression of the product nodes $\mathcal{P}(\mathcal{R}_p)$ corresponding to \mathcal{F} . Therefore, we use an *information bottleneck method* approach for learning the parameters [13]. Suppose we aim to merge \mathcal{R}_c to a region \mathcal{R}_p . Recalling the definition of the parts of a region

(Definition 7), the aim is to maximize the mutual information between the winner variable of \mathcal{R}_p and the winner variables of $\text{parts}(\mathcal{R}_p) := \{\mathcal{R}'_1, \dots, \mathcal{R}'_{|\text{parts}(\mathcal{R}_p)|}\}$, i.e.

$$\underset{\{w_{k,f}\}}{\text{maximize}} I(W_{\mathcal{R}'_1}, \dots, W_{\mathcal{R}'_{|\text{parts}(\mathcal{R}_p)|}}; W_{\mathcal{R}_p}) \quad (6)$$

where $\{w_{k,f}\}$ are the weights of the sum node S_k , i.e.

$$S_k(\mathbf{e}) = \sum_{f: P_f \in \mathcal{P}(\mathcal{R}_p)} w_{k,f} P_f(\mathbf{e}). \quad (7)$$

The weights satisfy $\sum_{f=1}^{|\mathcal{P}(\mathcal{R}_p)|} w_{k,f} = 1$, $w_{k,f} \geq 0$. Since this problem can be expected to be NP-hard, we restrict ourselves to a greedy solution, outlined in Algorithm 3. Our method starts with a number of sum nodes identical to the number of product nodes $\mathcal{P}(\mathcal{R})$, where each product node is the child of exactly one sum node. The weights are all initialized to 1, due to the normalization constraints. Then we iteratively combine a pair of sum nodes to a single sum node, such that the objective function (6) is maximized in each iteration; The weights of the new sum node are updated according to the maximum likelihood estimate

$$w_{k,f} = \frac{\sum_{m=1}^M P_f(\mathbf{e}^m)}{\sum_{f': P_{f'} \in \text{ch}(S_k)} \sum_{m=1}^M P_{f'}(\mathbf{e}^m)} \quad (8)$$

where \mathbf{e}^m denotes the input evidence of the m^{th} sample. Note that by this approach each product node becomes the child of exactly one sum node, i.e. the sum nodes have non-overlapping child sets.

Algorithm 3 Learn Parameters

- 1: For all product nodes P_i , $i = 1, \dots, |\mathcal{F}|$, with scope s , generate a sum node S_i in $\mathcal{R}_p := \mathcal{R}(s)$.
 - 2: Connect P_i as a child of S_i ; set $w_{i,i} = 1$.
 - 3: **while** number of sum nodes $> K$ **do**
 - 4: $I_{\text{best}} \leftarrow -\infty$
 - 5: **for** all pairs S_i, S_j of sum nodes in \mathcal{R}_p **do**
 - 6: Generate tentative sum node S_{tmp} .
 - 7: Connect $\text{ch}(S_i), \text{ch}(S_j)$ as children of S_{tmp} .
 - 8: Set weights of S_{tmp} according to (8).
 - 9: $\mathcal{R}_{\text{tmp}} \leftarrow S_{\text{tmp}} \cup \mathcal{R}_p \setminus \{S_i, S_j\}$.
 - 10: Estimate $I(W_{\mathcal{R}'_1}, \dots, W_{\mathcal{R}'_{|\text{parts}(\mathcal{R}_p)|}}; W_{\mathcal{R}_{\text{tmp}}})$.
 - 11: **if** $I(W_{\mathcal{R}'_1}, \dots, W_{\mathcal{R}'_{|\text{parts}(\mathcal{R}_p)|}}; W_{\mathcal{R}_{\text{tmp}}}) > I_{\text{best}}$ **then**
 - 12: $I_{\text{best}} = I(W_{\mathcal{R}'_1}, \dots, W_{\mathcal{R}'_{|\text{parts}(\mathcal{R}_p)|}}; W_{\mathcal{R}_{\text{tmp}}})$
 - 13: $\mathcal{R}_{\text{best}} = \mathcal{R}_{\text{tmp}}$
 - 14: **end if**
 - 15: **end for**
 - 16: $\mathcal{R}_p \leftarrow \mathcal{R}_{\text{best}}$
 - 17: **end while**
-

Algorithm 3 can be seen as a variant of the agglomerative information bottleneck method (AIB) [14]. To see this, note that in each iteration AIB merges two states of an RV X minimizing

$$I(g(X); X) - \beta I(g(X); Y) \quad (9)$$

over all functions g with a range of cardinality $|\mathbf{val}(X)| - 1$. Here, Y represents the relevant information and X the input data to be compressed. In other words, the AIB method performs compression (by minimizing the first term), while preserving relevant information (by maximizing the second term). In our case, the relevant information is the set of winner variables of the parts of \mathcal{R}_p , i.e. $W_{\mathcal{R}'_1}, \dots, W_{\mathcal{R}'_{|\text{parts}(\mathcal{R}_p)|}}$. The input data X is the winner variable $W_{\mathcal{R}_p}$ before merging two sum nodes. The difference to AIB is that we do not merge *states* of the winner variable $W_{\mathcal{R}_p}$, i.e. the relationship between two versions of the winner variable $W_{\mathcal{R}_p}$ in consecutive iterations of Algorithm 3 is not *functional*. Instead, each merge of two sum nodes leads to an update of the weights, and a node which was a winner for a given input \mathbf{x} need not remain the winner after the merge³. The joint distribution of the winner variables $\mathcal{R}'_1, \dots, \mathcal{R}'_{|\text{parts}(\mathcal{R}_p)|}, \mathcal{R}_p$ changes. By using the fixed weight training according to (8), our algorithm only has to optimize over $\frac{(|\mathcal{R}_p|-1)|\mathcal{R}_p|}{2}$ possible mappings⁴. Finally, our algorithm focuses on preserving relevant information, i.e. we set $\beta = \infty$ which aims to preserve a maximum amount of mutual information between the parent region and its parts.

In this paper, we simply set K to a fixed value. However, [14] suggests a method to set K in data-driven way: Each merge will inevitably lead to a loss of information⁵ w.r.t. the relevant variables $W_{\mathcal{R}'_1}, \dots, W_{\mathcal{R}'_{|\text{parts}(\mathcal{R}_p)|}}$ – if for a specific number of sum nodes a merge causes a loss which is high compared to the previous merges, this might suggest that a meaningful representation has been achieved. While previous merges eliminated mainly redundant information, any further merge would reduce the fidelity of the model significantly.

³ Indeed, if a sum node S_k not being merged was the winner for a given input \mathbf{x} , it will remain the winner even after merging two other sum nodes S_i and S_j . However, if one of the two sum nodes being merged won previously, the weight update may reduce the value of the merged sum node such that a different sum node, say S_k , wins for the input \mathbf{x} .

⁴ From a communication systems point-of-view, one can interpret this as a cascade of noisy communication channels, where each channel is represented by a stochastic matrix which reduces the cardinality of the alphabet by one. At each channel output one has the option of choosing among a set of further channels, until the desired output alphabet size is achieved. The vital part is that not always the best channel has to be chosen (i.e., the one with the maximum *capacity*), but rather the channel which best transfers the desired information. As such, it might even happen that the optimal channel has a small $I(W_{\mathcal{R}_p}; W_{\mathcal{R}_{lmp}})$; due to previous stochastic mappings (or *noisy channels*), $W_{\mathcal{R}_p}$ might contain *irrelevance*, which one of the following channels could successfully remove.

⁵ This rather informal formulation about information loss can be made rigorous; for a recent effort see [15].

4 Experiments

Poon and Domingos [1] demonstrated that SPNs achieve astonishing results on the ill-posed problem of image completion, i.e. reconstructing occluded parts of face images. To this end, they trained SPNs on the ORL face image data set [16] and used MPE-inference (*most probable explanation*) to recover missing pixel values, i.e. they inferred the most likely states of the occluded pixels and the states of the latent variables represented by sum nodes. MPE-inference is efficient in SPNs and serves as an approximation for MAP-inference, which actually is appropriate for this task. We conjecture that, although marginalization and MPE-inference is easy in SPNs, the exact MAP-problem is still intractable, since MAP is inherently harder than MPE [17]. However, proving or disproving this conjecture is future work and out of the scope of this paper.

We trained SPNs with the method by Poon and Domingos (PD) [1], the method by Dennis and Ventura (DV) [7], and our method (Merge). As in PD and DV, we model single pixels with several Gaussian nodes, where the means are set by the averages of histogram quantiles, and the standard deviation is uniformly set to 1. Using the notions introduced in this paper, this means that single pixels are used as atomic regions, containing a set of Gaussian nodes. The ORL faces contain 64×64 -pixels, which yields more than 8 million evaluations of the BD score (5) in the first iteration. Although we cache evaluations of the BD score, the computational effort is still large. Therefore, although we emphasize in this paper that our algorithm does not need prior knowledge of the problem domain, we use a similar approach as the PD algorithm, and introduce a “coarser” resolution level. We show the advantage of our algorithm, when no prior knowledge can be assumed, in the experiment following below.

To find the coarse resolution level, we apply affinity propagation [18] on the absolute value of the correlation coefficient matrix of the pixels, calculated on the training set. This process performs an unsupervised segmentation into atomic regions, which is shown in Figure 4. Within each atomic region, we train a



Fig. 4. Result of unsupervised segmentation of ORL faces using affinity propagation on the absolute value of correlation coefficients between pixels.

multi-root SPN with 20 roots using our Merge algorithm; these 20 roots serve in turn as atomic distributions for the overall Merge learning. Within each region,

pixels are treated as atomic regions, similar as in [1, 7]. For each application of Merge learning, we used a single tree-growing iteration. In this experiment, we set $G = 10$ for all three algorithms. As in [1, 7] we use $K = 20$ sum nodes per composite region for all algorithms. Figure 5 shows results on the face image completion task for PD, DV, and Merge. All three algorithms show convincing

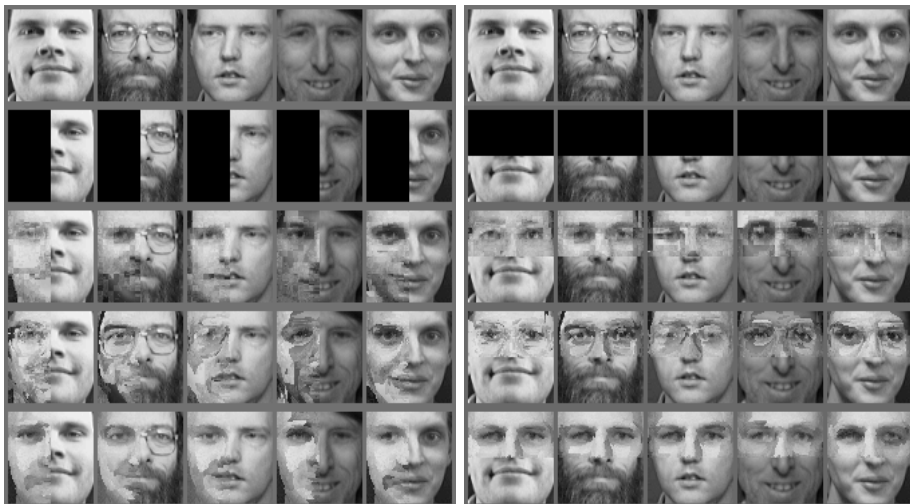


Fig. 5. Examples of face image reconstructions using MPE-inference. Rows from top to bottom: original image, covered image, PD [1], DV [7], Merge learning (this paper).

results but differ in the artifacts they produce. In Table 1 we summarize objective evaluation measures for this learning task; the signal-to-noise ratios show that Merge competes well with PD and DV, although no clear preference can be shown. However, we see that while Merge achieves the lowest training likelihood, it achieves the *highest* likelihood on the test set, stating that Merge generalized best in this task, i.e. it seems to be more robust against overfitting.

Table 1. Evaluation measures on ORL data. Left: reconstruction SNRs for the top, bottom, left, and right halves of face images covered. Right: Log-likelihoods on training and test set, normalized by number of samples.

	top	bottom	left	right	Train	Test
PD	12.34	10.18	11.58	11.72	-4290.46	-5071.61
DV	11.69	9.29	10.43	10.83	-4358.78	-4676.10
Merge	12.43	9.83	10.96	11.78	-4493.46	-4667.04

In this first experiment we used prior knowledge about the problem domain, by using AP for segmenting the image into atomic regions. To demonstrate that

our method does not rely on the incorporation of prior knowledge, we generated an artificial modification of the ORL data set; First, we rescale the ORL images to size 16×16 , yielding 256 variables. As in [7], we permute all pixels, i.e. we destroy the neighborhood information. Next, we discretized all pixels into 10 histogram bins and permute these randomly, i.e. we destroy the connection of the RVs by their value. Then we again performed the same experiment as with the large ORL data, where for each method we again used 10 Gaussian nodes per pixel, setting their means on the discretized values of bins 1 – 10, and setting the standard deviation uniformly to 1. Table 2 shows the result for the modified ORL data. We now see a clear trend: PD, relying on locality shows consistently the worst SNRs in the image reconstruction task. DV, not relying on locality, but on similar value trends, is consistently better than PD. Merge shows consistently the best SNRs. Similarly, looking at the log-likelihoods, we see that Merge shows the best test likelihood, i.e. it generalizes best in this task.

Table 2. Evaluation measures on down-scaled and permuted ORL data. Left: reconstruction SNRs for the top, bottom, left, and right halves of face images covered. Right: Log-likelihoods on training and test set, normalized by number of samples.

	top	bottom	left	right	Train	Test
PD	15.16	8.49	12.11	10.37	-443.41	-893.82
DV	15.32	9.24	12.62	10.55	-506.97	-623.22
Merge	17.95	10.53	13.22	12.48	-551.97	-595.66

5 Conclusion

In this paper, we introduced a method to learn SPNs in a greedy bottom-up manner, giving an alternative to the top-down approaches proposed so far. The main principle we follow is that SPNs simply build composite and complex models out of simple and small models in a *recursive* manner. The basis of this recursive principle is given by what we call *atomic* or input distributions. We adopted the notion of *regions* and interpret them as dictionaries of distributions over the same scope. Product nodes or partitions serve as *cross-overs* of dictionaries with non-overlapping scope, corresponding to the notion of decomposability. These cross-overs yield a quickly growing number of new features or product nodes. Sum nodes of the newly created region serve as *compression* of these newly created features. This process can be seen as *abstracting* information, when proceeding to higher levels.

We showed that our method competes well with existing generative approaches to train SPNs. Furthermore, we demonstrated that our method does not rely on assumptions of the image domain, and shows the best performance when these are not fulfilled. In future work, we want to explore potential engineering applications for our approach, such as signal, speech and audio processing.

Furthermore, we consider the discriminative paradigm, e.g. applying maximum margin methods for classification. Finally, we want to investigate different structure and parameter learning techniques within our learning framework.

References

1. Poon, H., Domingos, P.: Sum-product networks: A new deep architecture. In: Proceedings of the Twenty-Seventh Conference on Uncertainty in Artificial Intelligence. (2011)
2. Darwiche, A.: A differential approach to inference in bayesian networks. *ACM* **50**(3) (2003) 280–305
3. Lowd, D., Domingos, P.: Learning arithmetic circuits. In: Twenty Fourth Conference on Uncertainty in Artificial Intelligence. (2008) 383–392
4. Poon, H., Domingos, P.: <http://alchemy.cs.washington.edu/spn/> (2011) (online).
5. Gens, R., Domingos, P.: Discriminative learning of sum-product networks. In: Advances in Neural Information Processing Systems 25. (2012)
6. Coates, A., Lee, H., Ng, A.: An analysis of single-layer networks in unsupervised feature learning. In: Proceedings of the 14th International Conference on Artificial Intelligence and Statistics. (2011)
7. Dennis, A., Ventura, D.: Learning the architecture of sum-product networks using clustering on variables. In: Advances in Neural Information Processing Systems 25. (2012)
8. Hinton, G., Salakhutdinov, R.: Reducing the dimensionality of data with neural networks. *Science* **313**(5786) (2006) 504–507
9. Bengio, Y., Lamblin, P., Popovici, D., Larochelle, H.: Greedy layer-wise training of deep networks. In: Advances in Neural Information Processing Systems 19. (2007) 153–160
10. Bengio, Y.: Learning Deep Architectures for AI. Volume 2 of Foundations and Trends in Machine Learning. (2009)
11. Koller, D., Friedman, N.: Probabilistic Graphical Models: Principles and Techniques. MIT Press (2009)
12. Margaritis, D., Thrun, S.: A bayesian multiresolution independence test for continuous variables. In: 17th Conference on Uncertainty in Artificial Intelligence. (2001) 346–353
13. Tishby, N., Pereira, F.C., Bialek, W.: The information bottleneck method. In: Proc. Allerton Conf. on Communication, Control, and Computing. (September 1999) 368–377
14. Slonim, N., Tishby, N.: Agglomerative information bottleneck. In: Advances in Neural Information Processing Systems (NIPS), MIT Press (1999) 617–623
15. Geiger, B.C., Kubin, G.: Signal enhancement as minimization of relevant information loss. In: Proc. ITG Conf. on Systems, Communication and Coding, Munich (January 2013) 1–6 extended version available: [arXiv:1205.6935](https://arxiv.org/abs/1205.6935) [cs.IT].
16. Samaria, F., Harter, A.: Parameterisation of a stochastic model for human face identification. In: Proceedings of the 2nd IEEE Workshop on Applications of Computer Vision. (1994) 138–142
17. Park, J.: Map complexity results and approximation methods. In: Proceedings of the Conference on Uncertainty in Artificial Intelligence. (2002) 338–396
18. Frey, B., Dueck, D.: Clustering by passing messages between data points. *Science* **315** (2007) 972–976